Synthesis and evaluation of quinonoid compounds against tumor cell lines

ARTICLE *in* EUROPEAN JOURNAL OF MEDICINAL CHEMISTRY · JANUARY 2011

Impact Factor: 3.45 · DOI: 10.1016/j.ejmech.2010.11.006 · Source: PubMed

13 AUTHORS, INCLUDING:

Eufrânio N da Silva
Federal University of Minas Gerais
4 PUBLICATIONS **109** CITATIONS
SEE PROFILE

Carlos Kleber Z Andrade
University of Brasília
73 PUBLICATIONS **677** CITATIONS
SEE PROFILE

Carlos Alberto de Simone
University of São Paulo
122 PUBLICATIONS **830** CITATIONS
SEE PROFILE

Marília O F Goulart
Universidade Federal de Alagoas
161 PUBLICATIONS **2,147** CITATIONS
SEE PROFILE

European Journal of Medicinal Chemistry 46 (2011) 399–410

Contents lists available at ScienceDirect

European Journal of Medicinal Chemistry

journal homepage: http://www.elsevier.com/locate/ejmech

Short communication

Synthesis and evaluation of quinonoid compounds against tumor cell lines

Eufrânio N. da Silva Jr. [a,c,*], Bruno C. Cavalcanti [b], Tiago T. Guimarães [a], Maria do Carmo F.R. Pinto [a], Igor O. Cabral [b], Cláudia Pessoa [b], Letícia V. Costa-Lotufo [b], Manoel O. de Moraes [b], Carlos K.Z. de Andrade [c], Marcelo R. dos Santos [c], Carlos A. de Simone [e], Marilia O.F. Goulart [d], Antonio V. Pinto [a,1]

[a] Núcleo de Pesquisas de Produtos Naturais, UFRJ, 21941-971, Rio de Janeiro, RJ, Brazil
[b] Universidade Federal do Ceará, Departamento de Fisiologia e Farmacologia, Campus do Porangabussu, 60430-270 Fortaleza, CE, Brazil
[c] Instituto de Química, Universidade de Brasília, 70910-970 Brasília, DF, Brazil
[d] Instituto de Química e Biotecnologia, UFAL, Tabuleiro do Martins, 57072-970 Maceió, AL, Brazil
[e] Departamento de Física e Informática, Instituto de Física, USP, 13560-970 São Carlos, SP, Brazil

ARTICLE INFO

Article history:
Received 29 September 2010
Received in revised form
30 October 2010
Accepted 2 November 2010
Available online 9 November 2010

Keywords:
Naphthoquinones
Cancer
Cytotoxicity
Lapachol

ABSTRACT

Thirty two compounds were synthesized in moderate to high yields and showed activity against cancer cells HL-60 (leukemia), MDA-MB435 (melanoma), HCT-8 (colon) and SF295 (central nervous system), with IC_{50} below 2 μM for some compounds. The β-lapachone-based 1,2,3-triazoles showed the best cytoxicity profile and emerge as promising anticancer prototypes. Insights about the reactive oxygen species (ROS) mechanism of anticancer action for some compounds were obtained by addition of 1-bromoheptane that deplete reduced glutathione (GSH) content and by using N-acetylcysteine that protects cells against apoptotic cellular death, as well by analysis of thiobarbituric acid reactive substances (TBARS) formation, and oxidative DNA damage after treatment detected by the comet assay with the bacterial enzymes formamidopyrimidine DNA-glycosylase (FPG) and endonuclease III (ENDOIII).

1. Introduction

Naphthoquinones (NQs) have been the subject of much research due to their pharmacological activities [1–4].

Recently, shikonin, rhinacanthin and juglone derivatives [4–6], lapachol analogues [7,8], copper(II) complexes [9] obtained from lawsone have been described as antitumoral and are examples of the importance of natural products analogues as source of antitumoral compounds.

Several strategies are used to obtain new active compounds from natural products, as for instance, bioisosterism [10] and molecular hybridization [11] and in the last years the employment of click reactions [12] along with those strategies made possible the preparation of several heterocycles with antitumor activities [13].

Aiming to discover cytotoxic NQs, in the last few years, we have synthesized and evaluated the antitumor activity of naphthodihydrofuranquinones obtained from nor-lapachol, as for instance, nor-β-lapachone-based 1,2,3-triazoles [14], arylamino and alkoxy derivatives [15,16].

In continuity of our program for obtaining new substances from NQs with pharmacological activity, we prepared three classes of compounds. Recently, our research group, based on the studies of Ettlinger [17] and Anufriev [18], described the correct structure for Hooker's lapachol peroxide by X-ray crystallography [19]. Upon the use of this reaction, we synthesized the first class of compounds. Anthraquinone imidazoles constitute the second group and finally, using the approach of molecular hybridization [11], β-lapachone-based 1,2,3-triazoles, the third group, were prepared [20]. The trypanocidal activity against *Trypanosoma cruzi* of few of them has already been reported [20].

2. Chemistry

Lapachol (**1**) (2-hydroxy-3-(3′-methyl-2′-butenyl)-1,4-naphthoquinone) was extracted from the heartwood of *Tabebuia* sp. (*Tecoma*) and purified by a series of recrystallizations [21]. From this quinone, nor-lapachol (**2**) (2-hydroxy-3-(2′-methyl-propenyl)-1,4-naphthoquinone) was obtained by Hooker oxidation method [22].

The reduced quinones **7** and **9** synthesized from lapachol (**1**), **3** and **5** from nor-lapachol (**2**) and **13** and **15** from C-allyl lawsone (**11**)

* Corresponding author. Núcleo de Pesquisas de Produtos Naturais, UFRJ, 21944-971, Rio de Janeiro, RJ, Brazil. Tel.: +55 21 25626794; fax: +55 21 25626512.
E-mail address: eufranio.junior@yahoo.com.br (E.N. da Silva).
[1] In the memory of Professor Antonio Ventura Pinto due to his wonderful contribution for the accomplishment of this paper.

0223-5234/
doi:10.1016/j.ejmech.2010.11.006

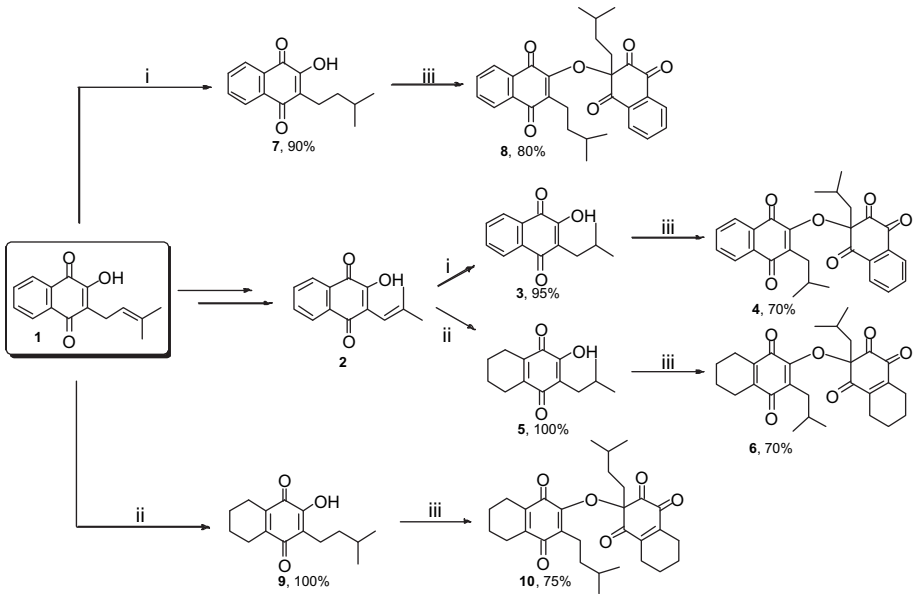

Scheme 1. Reagents and conditions: (i) EtOH, 10 mol % Pd/C, 30 psi of H_2, 15 min; (ii) AcOH, 10 mol % Pd/C, 55 psi of H_2, 6 h; (iii) AcOH, PbO_2.

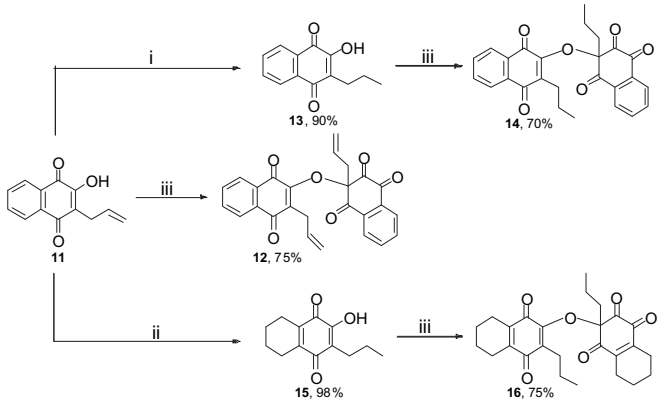

Scheme 2. Reagents and conditions: (i) EtOH, 10 mol % Pd/C, 30 psi of H_2, 15 min; (ii) AcOH, 10 mol % Pd/C, 55 psi of H_2, 6 h; (iii) AcOH, PbO_2.

were obtained by catalytic reduction with Pd/C used as catalyst. Using the Hooker's reaction with PbO_2 [19], these reduced compounds were used to prepare ether derivatives **4**, **6**, **8**, **10**, **12**, **14** and **16**, in good yields (Schemes 1 and 2). Syntheses of these ethers are easily accomplished by heating glacial acetic acid and lead dioxide. The reaction is finished in 2 min and after filtration to remove lead oxide, the products were purified by recrystallization and obtained as yellow crystals. Silica gel column chromatography should be avoided, once it favours the cleavage of the C–O–C bonds.

Finally, we applied the reaction of oxidative coupling with PbO_2 in phthiocol (Scheme 3) and an unexpected product **17** was obtained. Besides elucidating the structure by the use of

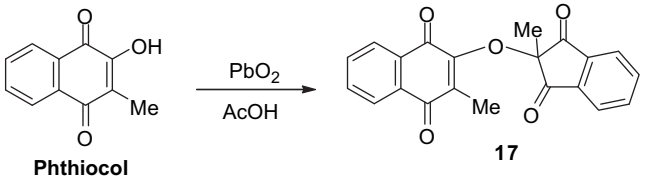

Scheme 3. Synthesis of compound **17**.

spectroscopic techniques, yellow crystals were obtained and the structure was reconfirmed by crystallographic methods. Ortep-3 diagram of the molecule is shown in Fig. 1, and Table 1 lists main crystallographic parameters.

The second series is constituted by anthraquinone imidazoles **18**–**28**. All the substances are herein described for the first time, except compounds **18** and **24** [20,23]. All of them are easily obtained from the reaction of 1,2-diaminoanthracene-9,10-dione (**17a**) and substituted aldehydes (Scheme 4).

The β-lapachone-based 1,2,3-triazoles **33**–**36** were synthesized as previously described [20]. These compounds were obtained from β-lapachone (**29**), synthesized by acid cyclisation of lapachol (**1**). N-bromosuccinimide (NBS) in CCl_4 with benzoyl peroxide as initiator were used to obtain 3,4-dibromo-β-lapachone (**30**) [24]. Substances **31** and **32** were separated by column chromatography and compound **32** was submitted to azide-alkyne Huisgen's cycloaddition catalysed by Cu(I) [25], producing the 1,2,3-triazoles **33**–**36** (Fig. 2).

The structures of compounds were confirmed by techniques such as ^1H and ^{13}C NMR, IR, high-resolution (electrospray ionization) mass spectra and spectroscopic data in comparison with related compounds [19,26]. Spectral data for the new ones are included.

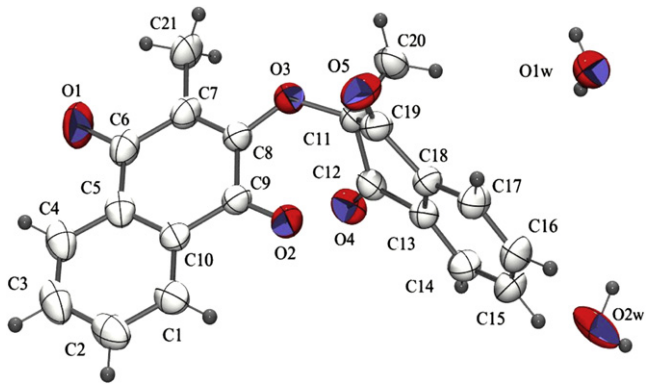

Fig. 1. An ORTEP-3 projection, showing the atomic labelling and the 50% probability ellipsoids of the compound **17**.

Table 1
Crystal data and structure refinement for compound **17**.

Empirical formula	$C_{21}H_{14}O_5 \cdot 2H_2O$
Formula weight	355.95
Temperature	298(2) K
Wavelength	0.71073 Å
Crystal system	Monoclinic
Space group	P 2_1/a
Unit cell dimensions	$a = 7.7078(3)$ Å $b = 19.9585(11)$ Å $c = 13.0416(6)$ Å
Volume	1978.02(10) Å^3
Z	4
Density (calculated)	1.19 mg/m^3
Absorption coefficient	0.086 mm^{-1}
F(000)	747
Crystal size	(0.242 × 0.225 × 0.132) mm^3
Theta range for data collection	3.0–25.7°
Index ranges	$9 \leq h \leq 9$
Reflections collected	15300
Independent reflections	3680 [R(int) = 0.115]
Completeness to theta	97.0%
Absorption correction	None
Max. and min. transmission	0.9913 and 0.9913
Refinement method	Full matrix least
Data/restraints/parameters	2171/0/255
Goodness-of-fit on F^2	1.024
Final R indices [I > 2sigma(I)]	R1 = 0.079, wR2 = 0.130
R indices (all data)	R1 = 0.222, wR2 = 0.272
Largest diff. peak and hole	0.378 and −0.255 e Å^{-3}

3. Results and discussion

All the substances herein described, except compounds **1**, **2**, **11**, **17a** and **30**, were evaluated in vitro against four cancer cell lines HL-60 (leukemia), MDA-MB435 (melanoma), HCT-8 (colon) and SF295 (central nervous system). Doxorubicin was used as the positive control, based on the MTT assay (Table 2) [27]. The selectivity of compounds toward a normal proliferating cell was investigated using the Alamar Blue assay performed with peripheral blood mononucluear cells (PBMC) after 72 h of drug exposure. Following Pérez-Sacau et al. [7] the compounds were classified according to their activity as highly active ($IC_{50} < 2$ μM), moderately active (2μM < $IC_{50} < 10$ μM), or inactive ($IC_{50} > 10$ μM).

Despite positive results in terms of antitumor activity [7,28,29] reduced compounds **3**, **5**, **7**, **9**, **13** and hybrid imidazoles were inactive. However, antitumoral activity against the evaluated cancer cell lines was evidenced for all 1,2,3-triazole derivatives (**33**–**36**) and intermediates **31** and **32**. The most significant activity was observed toward HL-60 and the compounds **32**, **33** and **35** were highly active with IC_{50} values of 1.43, 1.01 and 1.20 μM, respectively. Considering this cell line, these substances are as active as the prototype, β-lapachone (**29**) ($IC_{50} = 1.65$ μM).

For MDA-MB435, the activity of compounds **33**–**36** was significant with IC_{50} values below 2 μM. Only substance **33** was considered highly active against HCT-8 cell lines with IC_{50} value of 1.37 μM. Against SF295 all the substances presented values within the range 1.55–3.01 μM.

The most important cytotoxic mechanisms of quinonoid compounds involve drug bioreduction, followed by reaction with molecular oxygen and generation of ROS [1,29,30], and DNA damage is considered to be the most serious ROS-induced cellular modifications [31].

In fact, many of the effects of the chemical and physical agents that are commonly used in the treatment of human malignancies are mediated by induction of apoptosis. Nowadays, apoptosis has currently been a target for developing antitumor drugs [32]. To determine whether ROS are involved with quinonoid compounds-induced cell death, cultures were pre-treated with 1-bromoheptane, a non-toxic reduced glutathione (GSH) depleting agent [33] or pre-exposed to N-acetylcysteine (NAC), a widely used thiol-containing antioxidant that is a precursor of GSH which protects against oxidative stress-induced cell death by interacting with HO• and H_2O_2 [34]. Cell viability, morphological characterization of apoptotic cancer cells, lipid peroxidation, and DNA-damaging activities (i.e. DNA strand breaks and oxidized bases at the single-cell level) were monitored after cell treatment with some representatives of the above described three classes of compounds.

Cell membranes are often permeable to NQs, which, once, present in cell, may form adducts with DNA, leading to abasic sites and single or double strand breaks [35]. Initially, we correlated the ability of the precursor molecules β- and nor-β-lapachone to induce DNA strand breaks *via* intracellular ROS generation (Table 3), highlighting the great importance of the production of ROS on the antiproliferative effects of these NQs. Structure modifications at the level of nucleotidic bases can also occur as a consequence of oxidative stress. Oxidation of nucleotidic bases is likely to be as important as DNA strand breaks to overall cellular function and survival [36]. The most commonly used endonucleases in the modified comet assay are formamidopyrimidine

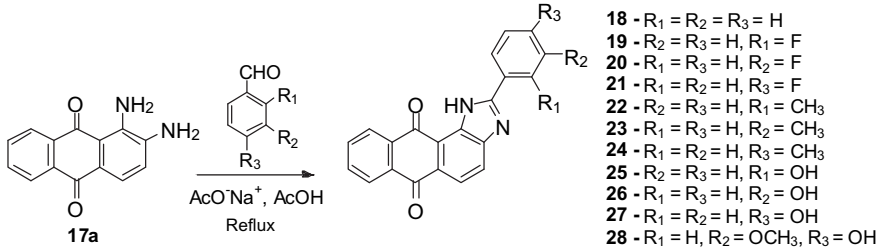

Scheme 4. Synthetic route for the preparation of imidazolic anthraquinones **18**–**28**.

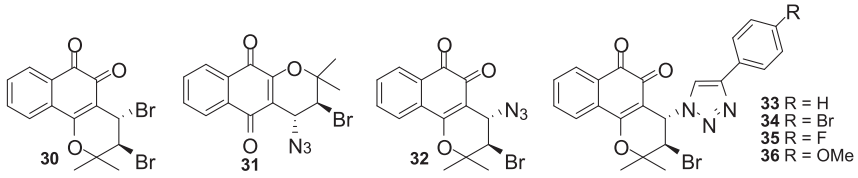

Fig. 2. Compounds **30**–**32** and β-Lapachone-based 1,2,3-triazoles **33**–**36** obtained from β-lapachone (**29**).

Table 2
Cytotoxic activity expressed by IC_{50} (μM) (95% CI) of compounds for cancer cell lines, obtained by nonlinear regression for all cell lines from three independent experiments.[a]

Compounds	IC_{50} (μM) (CI 95%)				
	PBMC	HL-60	MDA-MB435	HCT-8	SF295
3	>21.71	>21.71	>21.71	>21.71	>21.71
4	>10.91	>10.91	>10.91	>10.91	>10.91
5	>21.35	>21.35	>21.35	>21.35	>21.35
6	>10.72	>10.72	>10.72	>10.72	>10.72
7	>20.46	>20.46	>20.46	>20.46	>20.46
8	>10.27	>10.27	>10.27	>10.27	>10.27
9	>20.13	>20.13	>20.13	>20.13	>20.13
10	>10.10	>10.10	>10.10	>10.10	>10.10
12	>11.72	>11.72	>11.72	>11.72	>11.72
13	>23.12	>23.12	>23.12	>23.12	>23.12
14	>11.61	>11.61	>11.61	>11.61	>11.61
15	>22.70	>22.70	>22.70	3.99 (2.54–6.31)	>22.70
16	>11.40	>11.40	>11.40	>11.40	>11.40
17	>14.43	>14.43	>14.43	>14.43	>14.43
18	>15.41	>15.41	>15.41	>15.41	>15.41
19	>14.60	>14.60	>14.60	>14.60	>14.60
20	>14.60	>14.60	>14.60	>14.60	>14.60
21	>14.60	>14.60	>14.60	>14.60	>14.60
22	>14.77	>14.77	>14.77	>14.77	>14.77
23	>14.77	>14.77	>14.77	>14.77	>14.77
24	>14.77	>14.77	>14.77	>14.77	>14.77
25	>14.69	>14.69	>14.69	3.64 (2.90–4.55)	3.87 (2.99–5.02)
26	>14.69	>14.69	>14.69	>14.69	>14.69
27	>14.69	>14.69	>14.69	>14.69	>14.69
28	>13.61	>13.61	>13.61	>13.61	>13.61
31	11.3 (9.74–13.17)	5.68 (5.13–7.97)	3.97 (3.23–4.91)	12.39 (11.20–13.72)	>13.80
32	3.58 (3.34–3.86)	1.43 (1.32–1.54)	1.54 (1.46–1.62)	2.42 (2.31–2.54)	1.93 (1.76–2.12)
33	2.08 (1.80–2.41)	1.01 (0.92–1.11)	1.22 (0.88–1.74)	1.37 (1.27–1.50)	1.55 (1.20–1.55)
34	4.01 (3.53–4.49)	1.67 (1.56–1.82)	1.99 (1.74–2.31)	2.24 (2.11–2.41)	2.33 (2.02–2.72)
35	3.37 (3.00–3.81)	1.20 (1.03–1.38)	1.20 (1.03–1.40)	2.26 (2.13–2.40)	1.76 (1.47–2.11)
36	2.52 (2.16–2.95)	1.88 (1.69–2.08)	1.92 (1.61–2.28)	3.21(2.89–3.60)	3.01 (2.32–3.88)
Hooker's 'lapachol peroxide'[b] 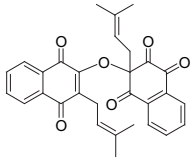	>10.36	>10.36	>10.36	9.76 (7.10–13.40)	>10.36
β-lapachone[c]	>20.6	1.65 (1.49–1.78)	0.25 (0.16–0.33)	0.83 (0.74–0.87)	0.91 (0.74–1.11)
Nor-β-lapachone[c]	>21.9	1.75 (nd)	0.31 (0.22–0.39)	1.36 (1.18–1.53)	1.58(1.31–1.88)
Doxorubicin[c]	0.42 (0.18–0.69)	0.03 (0.02–0.04)	0.88 (0.62–1.21)	0.06 (0.04–0.08)	0.41 (0.29–0.44)

[a] Alamar Blue assay was performed with human peripheral blood mononuclear cells (PBMC) after 72 h of drug exposure. Nd: not determined.
[b] Ref. [19].
[c] Refs. [15,16].

DNA-glycosylase (FPG, also known as MutM), and endonuclease III (ENDOIII, also known as NTH). FPG is specific for oxidized purines, specially for 8-oxo-7,8-dihydroguanine (8-oxoGua), and ENDOIII recognizes oxidized pyrimidines, including thymine glycol and uracil glycol [37].

Fig. 3 shows mean DNA damage caused by tested compounds, expressed as DNA damage index after treatment with DNA-repair enzymes ENDOIII and FPG. It was noted that the post-incubation results with the enzymes clearly show increased DNA migration of the compounds-treated human cancer cells cultures. The results indicate that the extent of oxidative DNA damage caused by compounds, as recognized by ENDOIII and FPG in cancer cells, was significantly higher. The present quinonoid compounds-generated ROS can attack DNA at both pyrimidine and purine bases, and lead to strand breaks. Based on these results, we suggest that active compounds facilitate DNA oxidative damage by ROS, such as

Table 3
Effects of β-lapachone and nor-β-lapachone on DNA damage index for 24 h using alkaline version of comet assay in the presence or absence of 5 mM NAC.

Compounds[a]	NAC[b]	DNA Damage index ± S.E.M			
		HL-60	MDA-MB435	HCT-8	SF295
β-lapachone	–	61.36 ± 4.15*	83.17 ± 3.25*	72.41 ± 2.56*	58.75 ± 1.15*
	+	8.33 ± 0.25	5.16 ± 0.10	11.41 ± 1.15	8.72 ± 2.25
Nor-β-lapachone	–	67.19 ± 0.96*	78.52 ± 1.11*	63.25 ± 3.25*	63.81 ± 0.75*
	+	12.36 ± 0.86	7.49 ± 0.33	10.48 ± 2.15	9.18 ± 0.56

*$p < 0.05$ compared to cultures treated in the presence of NAC by ANOVA/Tukey's test.
[a] Compounds were tested at 5 μM.
[b] N-acetylcysteine (NAC).

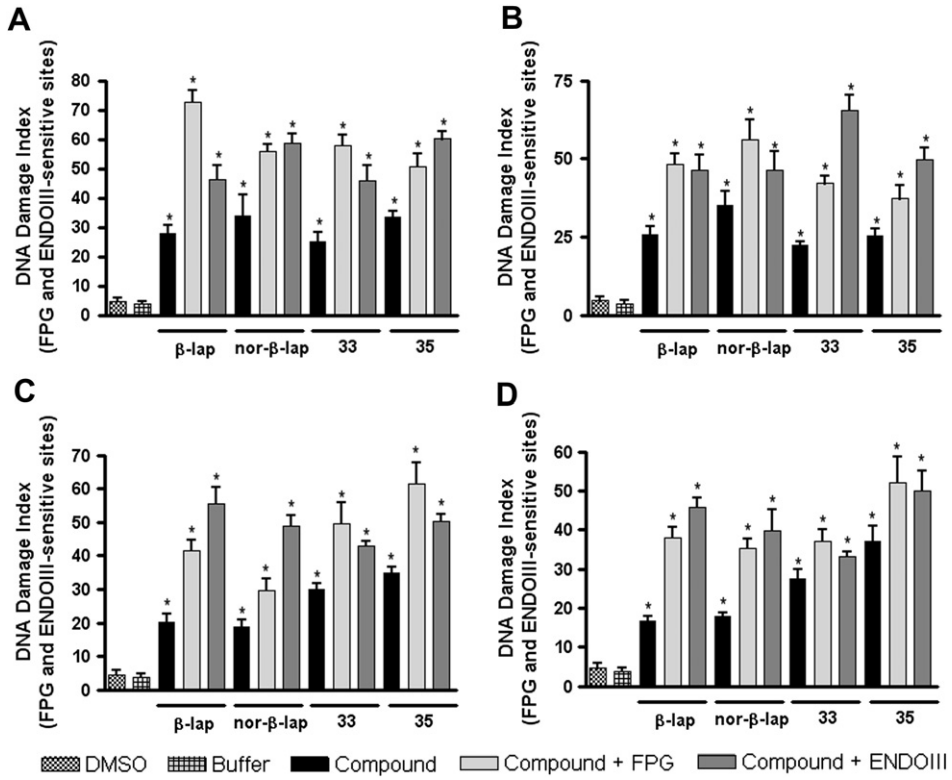

Fig. 3. Effects of FPG and ENDOIII on compounds (5 μM)-induced oxidative DNA damage after 12 h exposure by the alkaline version of the comet assay: HL-60 (**A**), MDA-MB435 (**B**), HCT-8 (**C**), and SF295 (**D**). Bars represent the mean ± S.E.M. of three independent experiments. $^{*}p < 0.05$ vs. DMSO (0.1%) by ANOVA/Tukey's test.

superoxide radical ($O_2^{\bullet -}$) and hydrogen peroxide (H_2O_2). H_2O_2 is not toxic by itself, but its high *in vivo* reactivity, through the Fenton reaction, where it reacts with partially reduced metal ions, generates hydroxyl radical ($HO^{\bullet}$), the most important radical in ROS-related DNA damage [38]. These radicals cause a variety of base lesions in DNA. In the case of tested compounds, the lesion produced is probably 8-oxoGua, the preferred substrate for FPG [39], and modified bases thymine glycol which is the more commonly recognized lesion by ENDOIII [40]. NQs also react with proteins and lipids, destroying their functionality, thereby causing cell death [41]. Therefore, in order to get additional evidences of the oxidative damage triggered by the present quinonoid compounds,

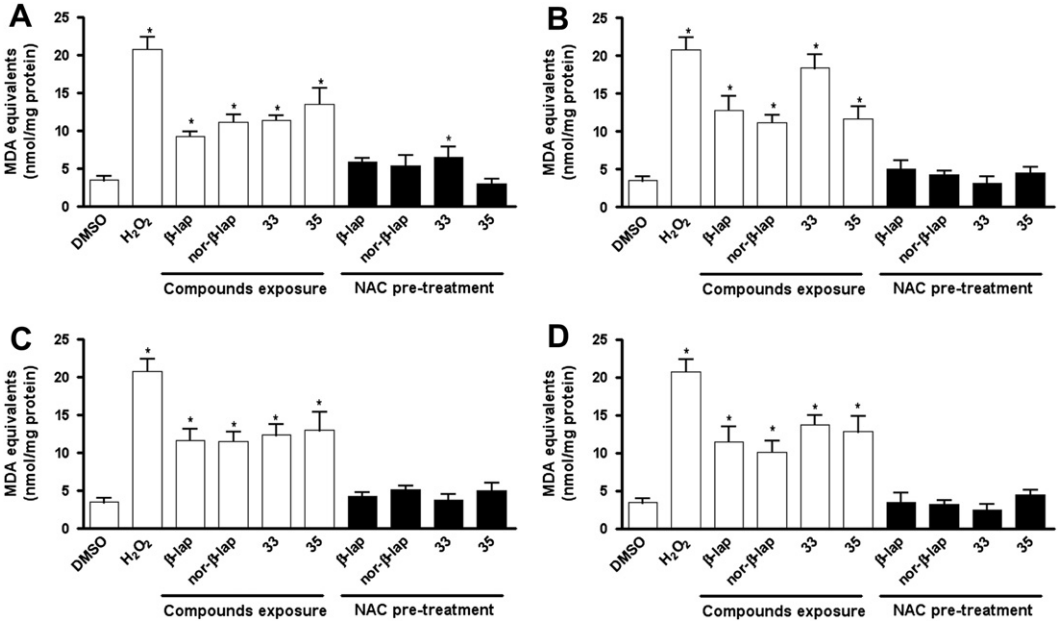

Fig. 4. Determination of TBARS of cancer cells [HL-60 (**A**), MDA-MB435 (**B**), HCT-8 (**C**), and SF295 (**D**)] exposed to compounds (5 μM) for 24 h. Open bars represent negative control (DMSO; 0.1%), H_2O_2 (10 μM for 2 h), or treatment with compounds. Filled bars represent the effect of pre-treatment with 5 mM N-acetylcysteine (NAC) added before compounds exposure. Bars represent the mean ± S.E.M. of three independent experiments. $^{*}p < 0.05$ vs. DMSO (0.1%) by ANOVA/Tukey's test.

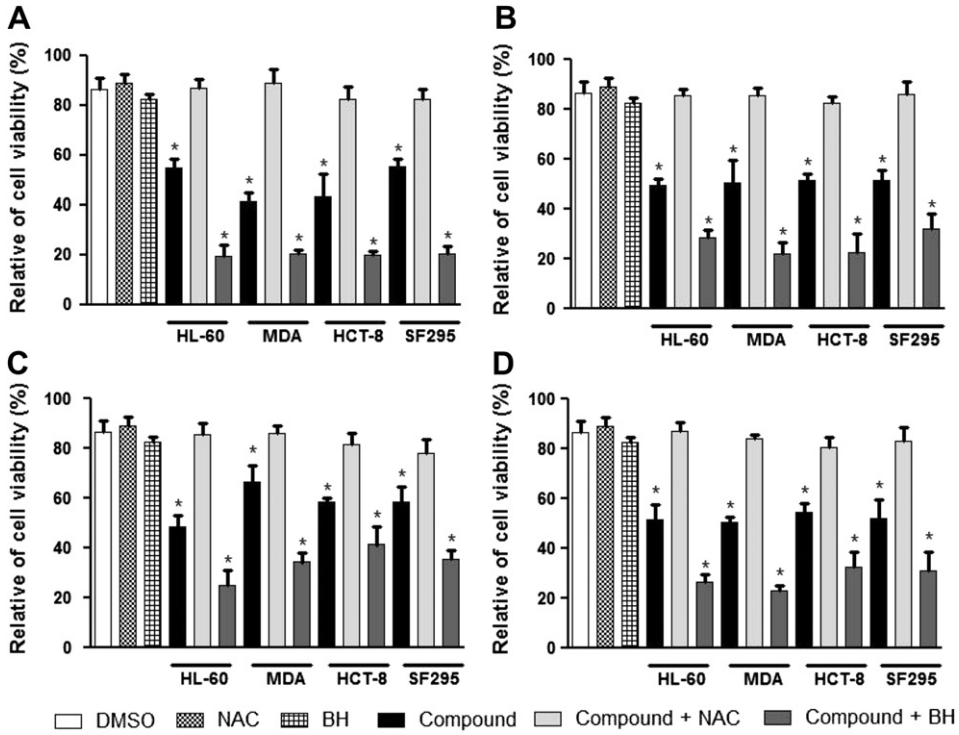

Fig. 5. Effects of compounds **33** (**A**), **35** (**B**), β-lapachone (**C**), and nor- β-lapachone (**D**) at 5 μM on cancer cell viability using trypan blue dye exclusion after 24 h of incubation in the presence or absence of 5 mM N-acetylcysteine (NAC) and 50 μM 1-bromoheptane (BH). Bars represent the mean ± S.E.M. of three independent experiments. *$p < 0.05$ *vs* DMSO (0.1%) by ANOVA/Tukey's test.

we examined the lipid peroxidation induced by these compounds. As seen in Fig. 4, the treatment of cancer cells with active substances resulted in an increase of TBARS formation. Pre-incubation with NAC prevented the quinonoid compounds-generated oxidative damage, as seen by the reduced level of TBARS.

These data corroborate other reports, which showed that β-lapachone, related compounds and other NQs induce ROS production and oxidative DNA damage [42].

Compounds **33** and **35** promoted cell death by apoptosis and genotoxicity [DNA strand breaks were reduced after pre-treatment

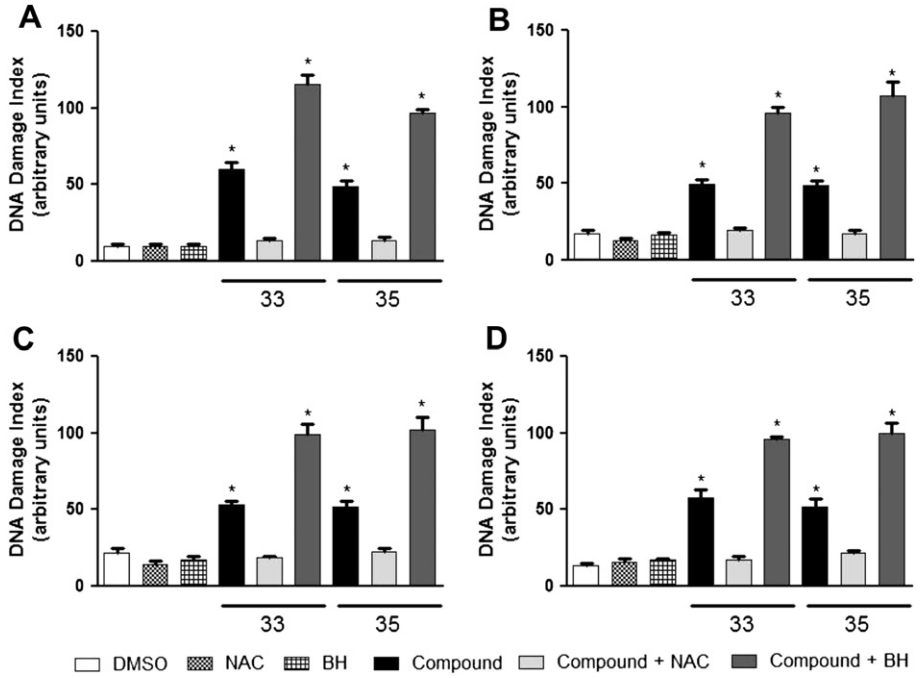

Fig. 6. Effect of compounds (**33** and **35**) at 5 μM on the induction of DNA strand breaks in human cancer cell lines after 24 h exposure by the alkaline version of the comet assay in the presence or absence of 5 mM N-acetylcysteine (NAC) and 50 μM 1-bromoheptane (BH): HL-60 (**A**), MDA-MB435 (**B**), HCT-8 (**C**), and SF295 (**D**). Bars represent the mean ± S.E.M. of three independent experiments. *$p < 0.05$ vs DMSO (0.1%) by ANOVA/Tukey's test.

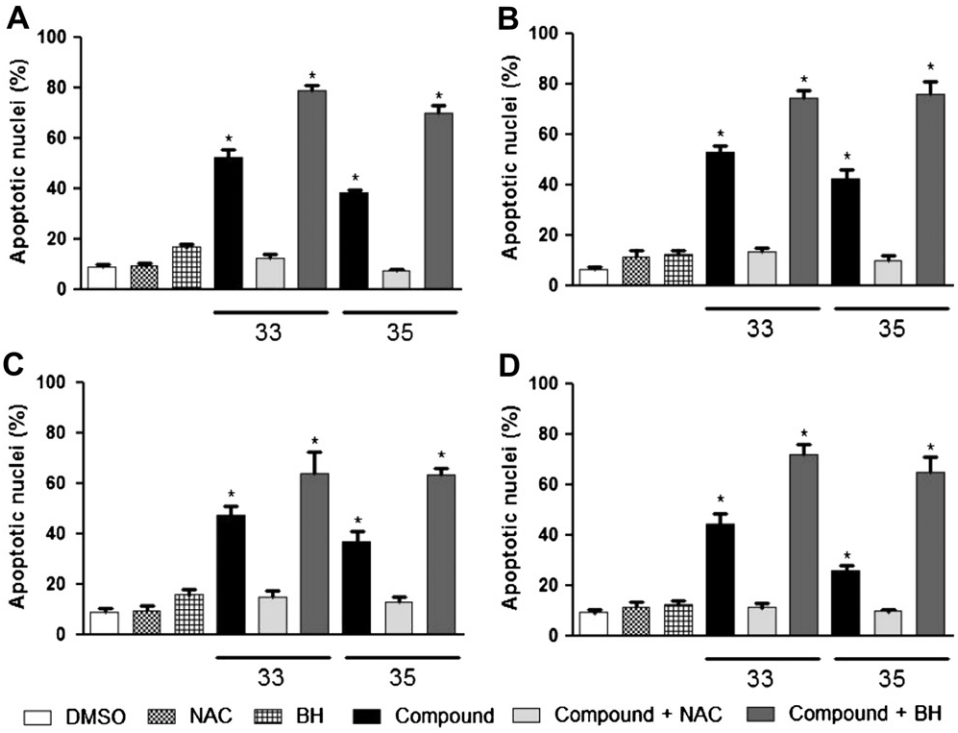

Fig. 7. Induction of cancer cells apoptosis by compounds (**33** and **35**) at 5 μM using acridine-orange and ethidium-bromide staining (AO/EB), and determined by fluorescence microscopy count after 24 h of incubation in the presence or absence of 5 mM N-acetylcysteine (NAC) and 50 μM 1-bromoheptane (BH): HL-60 (**A**), MDA-MB435 (**B**), HCT-8 (**C**), and SF295 (**D**). Bars represent the mean ± S.E.M. of three independent experiments. *$p < 0.05$ vs DMSO (0.1%) by ANOVA/Tukey's test.

Table 4
Effects of anthraquinone imidazoles, ethers quinones and Hooker's 'lapachol peroxide' on cancer cell apoptosis at 5 μM using acridine-orange and ethidium-bromide staining (AO/EB). Apoptotic nuclei were determined by fluorescence microscopy analysis after 24 h of exposure in the presence or absence 50 μM BH.

Compounds[a]	BH[b]	Apoptotic nuclei (%) ± S.E.M.			
		HL-60	MDA-MB435	HCT-8	SF295
H_2O_2[c]	–	83.17 ± 4.15*	74.59 ± 3.75*	80.66 ± 5.16*	85.03 ± 7.15*
18	+	8.37 ± 2.45	11.44 ± 0.81	8.11 ± 0.10	9.17 ± 0.96
	–	12.59 ± 4.10	9.02 ± 0.75	10.35 ± 0.10	7.32 ± 0.11
22	+	10.75 ± 0.56	10.38 ± 0.10	9.17 ± 1.45	13.95 ± 3.45
	–	11.47 ± 1.75	6.33 ± 0.33	5.33 ± 0.33	11.85 ± 0.81
23	+	6.18 ± 0.81	6.17 ± 0.56	7.28 ± 0.11	7.38 ± 1.15
	–	7.33 ± 1.17	9.81 ± 0.11	12.01 ± 0.10	10.05 ± 0.10
24	+	9.62 ± 0.56	12.27 ± 3.15	9.31 ± 0.33	4.17 ± 0.10
	–	5.27 ± 0.11	7.49 ± 0.25	8.72 ± 1.17	5.82 ± 0.10
25	+	12.59 ± 2.45	10.04 ± 0.21	4.19 ± 0.10	9.91 ± 0.75
	–	8.21 ± 0.75	7.39 ± 0.33	6.48 ± 0.56	11.73 ± 1.17
26	+	8.17 ± 0.33	13.75 ± 0.56	7.25 ± 0.45	9.66 ± 0.10
	–	10.49 ± 1.15	12.51 ± 0.10	12.73 ± 2.45	13.51 ± 3.15
27	+	14.26 ± 3.45	13.07 ± 1.15	11.16 ± 0.11	10.18 ± 0.56
	–	10.70 ± 2.08	9.56 ± 1.75	8.51 ± 0.75	5.93 ± 0.11
8	+	4.17 ± 0.11	7.44 ± 1.05	11.46 ± 0.10	8.01 ± 0.10
	–	8.13 ± 0.17	9.51 ± 1.25	8.71 ± 1.05	7.94 ± 0.56
10	+	10.62 ± 0.25	13.72 ± 2.45	10.33 ± 0.11	12.06 ± 2.25
	–	10.21 ± 1.15	8.38 ± 0.75	5.85 ± 0.25	8.33 ± 0.75
12	+	8.55 ± 0.11	11.36 ± 1.15	9.37 ± 0.15	11.47 ± 0.11
	–	3.91 ± 0.11	7.94 ± 0.10	12.52 ± 0.75	8.30 ± 0.10
16	+	11.04 ± 0.15	12.09 ± 2.45	11.70 ± 1.15	13.97 ± 0.33
	–	9.13 ± 3.15	8.56 ± 0.10	9.27 ± 0.11	11.73 ± 1.15
Hooker's 'lapachol peroxide'[d]	+	8.46 ± 0.15	5.82 ± 0.11	9.16 ± 0.33	7.30 ± 0.21
	–	11.17 ± 0.33	4.72 ± 0.25	8.52 ± 0.10	11.45 ± 0.15

*$p < 0.05$ compared to cultures treated in the presence or absence of BH by ANOVA/Tukey's test.
[a] Compounds were tested at 5 μM.
[b] 1-Bromoheptane (BH).
[c] H_2O_2 at 10 μM during 2 h.
[d] Ref. [19].

with NAC, which increase the percentage of viable cells (trypan blue stain)], suggesting that tested quinones-induced apoptosis is associated with ROS production (Figs. 5–7). Moreover, emphasizing the ROS contribution on the cellular toxicity, the GSH content was depleted by using a non-toxic concentration of 1-bromoheptane (trypan blue stain). In GSH-depleted cell cultures, an increase in cell death (% apoptotic nuclei) as well as in the levels of DNA strand breaks (comet assay), was observed.

The effects of anthraquinone imidazoles **18** and **22**–**27**, ethers quinones **8**, **10**, **12**, **16** and Hooker's 'lapachol peroxide' [19] (inactive compounds) on cancer cell apoptosis at 5 μM using DNA-binding fluorescent dye (AO/EB) staining (Table 4) showed that these substances do not generate ROS in this concentration, since the pre-treatment with 1-bromoheptane did not show any influence on the activity of these compounds. These data corroborate with the inactivity in cancer cell lines.

4. Conclusions

In this paper, we listed a series of new NQs that were evaluated against tumor cell lines. Only the β-lapachone-based 1,2,3-triazoles were highly active ($IC_{50} < 2$ μM) for cancer cell lines, for instance, HL-60 and MDA-MB435, inducing apoptotic cell death mediated by ROS generation, similarly to the precursor molecules. Thus, the β-lapachone-based 1,2,3-triazoles can be considered promising prototypes for cancer therapy.

5. Experimental

5.1. Chemistry

Melting points were obtained on Thomas Hoover and are uncorrected. Analytical grade solvents were used. Column chromatography was performed on silica gel (Acros Organics 0.035–

0.070 mm, pore diameter ca 6 nm). Infrared spectra were recorded on a Perkin–Elmer FT-IR Spectrometer. ^{1}H and ^{13}C NMR were recorded at room temperature using a Varian Mercury Plus 300 and Varian MR 400 instrument, in the solvents indicated, with TMS as internal standard. Chemical shifts (δ) are given in ppm and coupling constants (J) in Hertz. High-resolution mass spectra (electrospray ionization) were obtained using a MicroTOF Ic - Bruker Daltonics. All the compounds were nominated using the program CS ChemDraw Ultra version 5.0 and 10.0.

5.2. General procedures to prepare the ether-compounds

The hydroxyquinone in glacial acetic acid was heated to boiling, the source of heat was removed, and lead dioxide was added. The hot mixture was shaken for 2 min and filtered to remove lead oxide, and after precipitation on cooling, very slowly, and filtration, crystals of the ether were obtained [19].

5.2.1. 3-(3-Methyl-butyl)-3-[3-(3-methyl-butyl)-1,4-dioxo-1,4-dihydro-naphthalen-2-yloxy]-naphthalene-1,2,4-trione **8**

The reaction of 2-hydroxy-3-(3-methyl-butyl)-[1,4]naphthoquinone (**7**), (244 mg, 1 mmol), 2.5 mL of AcOH and 244 mg of PbO_2 yielded product **8**, (388 mg, 0.8 mmol, 80% yield) as an orange solid; mp 77–81 °C; IR (KBr) 1747 (C═O), 1697 (C═O), 1649 (C═O), 1593 (C═O), 1577 (C═O) cm^{-1}; ^{1}H NMR (300 MHz, $CDCl_3$) δ 8.44–8.41 (1H, m), 8.24–8.21 (1H, m), 8.04–8.00 (1H, m), 7.96–7.92 (2H, m), 7.67–7.62 (2H, m), 7.53–7.48 (1H, m), 2.82–2.77 (2H, m), 2.06–1.99 (2H, m), 1.78–1.25 (6H, m), 1.02 (6H, d, J = 6.4 Hz), 0.85–0.81 (6H, m); ^{13}C NMR (75 MHz, $CDCl_3$) δ 189.0 (C═O), 184.3 (C═O), 184.2 (C═O), 182.0 (C═O), 180.7 (C═O), 150.8, 136.1, 134.8, 134.4, 133.9, 133.6, 132.9, 131.6, 130.6, 129.0, 128.5, 126.5, 126.1, 93.1, 36.9, 35.5, 31.5, 28.8, 27.9, 22.5, 22.4, 22.2; EI/HRMS (m/z) $[M + H]^+$ 487.2124. Calcd for $[C_{30}H_{30}O_6H]^+$: 487.2121.

5.2.2. 3-(3-Methyl-butyl)-3-[3-(3-methyl-butyl)-1,4-dioxo-1,4,5,6,7,8-hexahydro-naphthalen-2-yloxy]-5,6,7,8-tetrahydro-naphthalene-1,2,4-trione **10**

The reaction of 2-hydroxy-3-(3-methyl-butyl)-5,6,7,8-tetrahydro-[1,4]naphthoquinone (**9**), (248 mg, 1 mmol), 2.5 mL of AcOH and 248 mg of PbO_2 yielded product **10**, (370 mg, 0.7 mmol, 75% yield) as an orange solid; mp 74–78 °C; IR (KBr) 1749 (C═O), 1683 (C═O), 1639 (C═O), 1604 (C═O) cm^{-1}; ^{1}H NMR (300 MHz, $CDCl_3$) δ 2.85–2.53 (4H, m), 2.20–1.15 (22H, m), 0.95 (6H, d, J = 6.4 Hz), 0.85 (6H, d, J = 6.4 Hz); ^{13}C NMR (75 MHz, $CDCl_3$) δ 190.5 (C═O), 187.1 (C═O), 184.4 (C═O), 184.1 (C═O), 182.1 (C═O), 149.3, 147.1, 143.2, 139.7, 129.5, 92.2, 37.2, 36.3, 32.0, 29.0, 28.2, 24.5, 23.4, 23.2, 23.0, 22.7, 22.5, 22.4, 22.3, 21.8, 21.2, 21.1, 21.0; EI/HRMS (m/z) $[M + H]^+$ 495.2731. Calcd for $[C_{30}H_{38}O_6H]^+$: 495.2747.

5.2.3. 3-Isobutyl-3-(3-isobutyl-1,4-dioxo-1,4-dihydro-naphthalen-2-yloxy)-naphthalene-1,2,4-trione **4**

The reaction of 2-hydroxy-3-isobutyl-[1,4]-naphthoquinone (**3**), (230 mg, 1 mmol), 2.5 mL of AcOH and 230 mg of PbO_2 yielded product **4**, (320 mg, 0.70 mmol, 70% yield) as an orange solid; mp 79–80 °C; IR (KBr) 1749 (C═O), 1701 (C═O), 1651 (C═O), 1593 (C═O), 1575 (C═O) cm^{-1}; ^{1}H NMR (300 MHz, $CDCl_3$) δ 8.43–8.40 (1H, m), 8.23–8.20 (1H, m), 8.05–8.01 (1H, m), 7.96–7.92 (2H, m), 7.68–7.62 (2H, m), 7.54–7.48 (1H, m), 2.74 (2H, d, J = 7.4 Hz), 2.31–1.94 (2H, m), 1.94 (2H, d, J = 7.4 Hz), 1.07 (3H, d, J = 1.6 Hz), 1.07 (3H, d, J = 1.6 Hz), 0.97 (3H, d, J = 6.5 Hz), 0.91 (3H, d, J = 6.5 Hz); ^{13}C NMR (75 MHz, $CDCl_3$) δ 188.8 (C═O), 184.5 (C═O), 184.3 (C═O), 182.1 (C═O), 181.0 (C═O), 151.3, 136.1, 134.7, 134.4, 134.1, 132.9, 132.8, 132.5, 131.5, 130.7, 129.0, 128.5, 126.5, 126.2, 94.0, 45.8, 32.8, 28.4, 24.0, 23.9, 23.1, 23.0; EI/HRMS (m/z) $[M + H]^+$ 459.1802. Calcd for $[C_{28}H_{26}O_6H]^+$: 459.1808.

5.2.4. 3-Isobutyl-3-(3-isobutyl-1,4-dioxo-1,4,5,6,7,8-hexahydro-naphthalen-2-yloxy)-5,6,7,8-tetrahydro-naphthalene-1,2,4-trione **6**

The reaction of 2-hydroxy-3-isobutyl-5,6,7,8-tetrahydro-[1,4]naphthoquinone (**5**), (234 mg, 1 mmol), 2.5 mL of AcOH and 234 mg of PbO_2 yielded product **6**, (326 mg, 0.7 mmol, 70% yield) as an orange solid; mp 78–82 °C; IR (KBr) 1749 (C═O), 1683 (C═O), 1641 (C═O), 1602 (C═O) cm^{-1}; ^{1}H NMR (300 MHz, $CDCl_3$) δ 2.84–2.61 (2H, m), 2.51–2.32 (5H, m), 2.20–2.04 (2H, m), 1.91–1.77 (6H, m), 1.66–1.51 (5H, m), 0.98 (3H, d, J = 1.8 Hz), 0.96 (3H, d, J = 1.8 Hz), 0.93 (3H, d, J = 6.5 Hz), 0.90 (3H, d, J = 6.5 Hz); ^{13}C NMR (75 MHz, $CDCl_3$) δ 190.0 (C═O), 187.1 (C═O), 184.0 (C═O), 183.8 (C═O), 182.1 (C═O), 149.2, 146.6, 142.7, 139.5, 128.1, 92.7, 46.6, 32.1, 28.2, 24.3, 23.9, 23.8, 23.0, 22.9, 22.0, 21.0, 20.8, 20.7; EI/HRMS (m/z) $[M + H]^+$ 467.2441. Calcd for $[C_{28}H_{34}O_6H]^+$: 467.2434.

5.2.5. 3-Allyl-3-(3-allyl-1,4-dioxo-1,4-dihydro-naphthalen-2-yloxy)-naphthalene-1,2,4-trione **12**

The reaction of 2-allyl-3-hydroxy-[1,4]naphthoquinone (**11**), (214 mg, 1 mmol), 2.5 mL of AcOH and 214 mg of PbO_2 yielded product **12**, (319 mg, 0.7 mmol, 70% yield) as an orange solid; mp 93–95 °C; IR (KBr) 1747 (C═O), 1699 (C═O), 1651 (C═O), 1591 (C═O), 1577 (C═O) cm^{-1}; ^{1}H NMR (300 MHz, $CDCl_3$) δ 8.45–8.39 (1H, m), 8.28–8.17 (1H, m), 8.06–8.01 (1H, m), 7.97–7.91 (2H, m), 7.70–7.63 (2H, m), 7.59–7.49 (1H, m), 6.08–5.95 (1H, m), 5.78–5.64 (1H, m), 5.35–5.27 (1H, m), 5.19–5.13 (2H, m), 5.12–5.05 (1H, m), 3.58–3.55 (2H, m), 2.85–2.82 (2H, m); ^{13}C NMR (75 MHz, $CDCl_3$) δ 188.5 (C═O), 184.0 (C═O), 183.6 (C═O), 182.0 (C═O), 180.0 (C═O), 150.0, 136.6, 134.9, 134.6, 133.8, 133.0, 131.3, 130.3, 130.0, 129.0, 128.3, 128.2, 126.4, 126.1, 126.1, 116.8, 92.7, 42.0, 27.9; EI/HRMS (m/z) $[M + H]^+$ 427.1175. Calcd for $[C_{26}H_{18}O_6H]^+$: 427.1182.

5.2.6. 3-(1,4-Dioxo-3-propyl-1,4-dihydro-naphthalen-2-yloxy)-3-propyl-naphthalene-1,2,4-trione **14**

The reaction of 2-hydroxy-3-propyl-[1,4]naphthoquinone (**13**), (216 mg, 1 mmol), 2.5 mL of AcOH and 216 mg of PbO_2 yielded product **14**, (301 mg, 0.7 mmol, 70% yield) as an orange solid; mp 89–91 °C; IR (KBr) 1747 (C═O), 1701 (C═O), 1651 (C═O), 1593 (C═O), 1577 (C═O) cm^{-1}; 1H NMR (300 MHz, $CDCl_3$) δ 8.43–7.48 (8H, m), 2.81–1.39 (8H, m), 1.08 (3H, t, J = 7.0 Hz), 0.91 (3H, t, J = 7.0 Hz); ^{13}C NMR (75 MHz, $CDCl_3$) δ: 192.3 (C═O), 189.0 (C═O), 184.4 (C═O), 184.3 (C═O), 182.1 (C═O), 151.0, 136.1, 135.0, 134.4, 134.0, 133.1, 133.0, 133.0, 131.6, 130.6, 129.0, 128.4, 126.5, 126.2, 93.2, 39.5, 26.1, 21.6, 16.6, 14.5, 14.0.

5.2.7. 3-(1,4-Dioxo-3-propyl-1,4,5,6,7,8-hexahydro-naphthalen-2-yloxy)-3-propyl-5,6,7,8-tetrahydro-naphthalene-1,2,4-trione **16**

The reaction of 2-hydroxy-3-propyl-5,6,7,8-tetrahydro-[1,4]naphthoquinone (**15**), (220 mg, 1 mmol), 2.5 mL of AcOH and 220 mg of PbO_2 yielded product **16**, (328 mg, 0.7 mmol, 70% yield) as an orange solid; mp 71–94 °C; IR (KBr) 1749 (C═O), 1683 (C═O), 1639 (C═O), 1604 (C═O) cm^{-1}; ^{1}H NMR (300 MHz, $CDCl_3$) δ 2.87–2.27 (8H, m), 2.16–1.25 (16H, m), 0.99 (3H, t, J = 7.0 Hz), 0.92 (3H, t, J = 7.0 Hz); ^{13}C NMR (75 MHz, $CDCl_3$) δ 190.5 (C═O), 187.2 (C═O), 184.1 (C═O), 183.0 (C═O), 182.0 (C═O), 149.4, 147.2, 143.1, 139.7, 129.1, 92.3, 40.2, 34.2, 25.6, 24.5, 23.4, 23.0, 22.3, 21.9, 21.2, 21.1, 21.0, 17.1, 14.6, 14.2; EI/HRMS (m/z) $[M + H]^+$ 439.2126. Calcd for $[C_{26}H_{30}O_6H]^+$: 439.2121.

5.2.8. 2-Methyl-3-(2-methyl-1,3-dioxo-indan-2-yloxy)-[1,4] naphthoquinone **17**

The reaction of 188 mg of phithiocol, 18.8 mL of AcOH and 188 mg of PbO_2 yielded the compound **17**, (311 mg, 0.9 mmol, 90% yield) as a yellow prisms; mp 152–153 °C; IR (KBr) 1754 (C═O), 1720 (C═O), 1655 (C═O), 1612 (C═O) cm^{-1}; ^{1}H NMR (300 MHz, $CDCl_3$) δ 8.07–8.00 (3H, m), 7.96–7.89 (2H, m), 7.67–7.60 (2H, m), 7.55–7.48 (1H, m), 2.27 (3H, s), 1.74 (3H, s); ^{13}C NMR (75 MHz,

$CDCl_3$) δ 195.5 (C═O), 184.9 (C═O), 181.1(C═O), 152.8, 138.6, 136.0, 134.2, 133.0, 132.0, 130.5, 130.3, 126.2, 124.1, 84.1, 23.4, 9.8. EI/HRMS (*m*/*z*) $[M + Na]^+$ 369.0717. Calcd for $[C_{21}H_{14}O_5Na]^+$: 369.0739.

5.3. General procedures to prepare the reduced compounds

3-Hydroxy-naphthoquinone was dissolved in the appropriate solvent and submitted to catalytic reduction over 10 mol% of the Pd/C as a catalyst. The reaction was monitored by TLC and after the complete consumption of the quinone reactant the reaction mixture was filtered and the product was purified by column chromatography in silica gel, eluted with an increasing polarity gradient mixture of hexane and ethyl acetate.

5.3.1. 2-Hydroxy-3-isobutyl-5,6,7,8-tetrahydro-[1,4] naphthoquinone **5**

Nor-lapachol (**2**), (228 mg, 1 mmol) in 15 mL of AcOH, 55 psi of H_2 and 10% of Pd/C during 6 h, yielded product **5**, (234 mg, 1 mmol, 100% yield) as a yellow solid; mp 88–90 °C; IR (KBr) 1647 (C═O), 1631 (C═O), 3369 (-OH) cm^{-1}; ^1H NMR (300 MHz, $CDCl_3$) δ 6.93 (OH, sl), 2.49–2.39 (4H, m), 2.31 (1H, d, *J* = 7.2 Hz), 1.92–1.79 (1H, m), 1.71–1.67 (4H, m), 0.89 (6H, d, *J* = 6.5 Hz); ^{13}C NMR (75 MHz, $CDCl_3$) δ 187.5 (C═O), 183.4 (C═O), 151.0, 145.0, 137.7, 120.0, 31.6, 27.9, 23.1, 22.6, 21.8, 21.1, 21.0; MS [70 eV, *m*/*z* (%)]: 115 (8), 192 (11), 65 (13), 91 (17), 234 (17), 79 (27), 41 (100).

5.3.2. 2-Hydroxy-3-propyl-5,6,7,8-tetrahydro-[1,4] naphthoquinone **15**

C-Allyl lawsone (**11**), (214 mg, 1 mmol) in 15 mL of AcOH, 55 psi of H_2 and 10% of Pd/C during 6 h, yielded product **15**, (220 mg, 0.98 mmol, 98% yield) as a yellow solid; mp 65–67 °C; IR (KBr) 1647 (C═O), 1618 (C═O) cm^{-1}; ^1H NMR (300 MHz, $CDCl_3$) δ 2.51–2.35 (6H, m), 1.74–1.65 (4H, m), 1.48 (2H, sextet, *J* = 7.5 Hz), 0.93 (1H, t, *J* = 7.4 Hz); ^{13}C NMR (75 MHz, $CDCl_3$) δ 187.7 (C═O), 183.8 (C═O), 151.0, 145.2, 137.9, 120.8, 25.0, 23.2, 22.1, 21.8, 21.4, 21.2, 14.3; MS [70 eV, *m*/*z* (%)]: 85 (70), 220 (80), 83 (100).

5.4. General procedure for the synthesis of the antraquinones

A solution of 1,2-diamino-anthraquinone (**17a**) (238 mg, 1 mmol) in 5 mL of AcOH, sodium acetate (106 mg, 1.3 mmol) and the desired aldehyde (see below) were stirred in reflux. TLC was used to monitor the end of the reaction. After the addition of water, the formed precipitate was filtered, and the product was purified by column chromatography using as eluent a mixture of dichloromethane/ethyl acetate (5:1).

5.4.1. 2-(2-Fluorophenyl)-1H-anthra[1,2-d]imidazole-6,11-dione **19**

From 2-fluoro-benzaldehyde (136 mg, 1.1 mmol), **19** was obtained as a yellow solid (207 mg, 0.61 mmol, 61% yield, mp 290–291 °C).

IR (KBr) 3450, 1668, 1583, 1489, 1465, 1436, 1328, 1290, 1271, 765, 715, 605 cm^{-1} ^1H NMR (400 MHz, DMSO-d_6) δ 11.81–11.64 (m, 1H), 8.54 (t, *J* = 7.79 Hz, 1H), 8.38–8.34 (m, 1H), 8.34–8.30 (m, 1H), 8.27 (d, *J* = 8.40 Hz, 1H), 8.16 (d, *J* = 8.39 Hz, 1H), 7.85–7.79 (m, 2H), 7.61–7.51 (m, 1H), 7.42–7.29 (m, 2H). ^{13}C NMR (75 MHz, DMSO-d_6) δ 183.5, 182.8, 164.5, 156.8, 134.9, 134.8, 133.4, 131.7, 131.6, 131.5, 131.4, 131.3, 128.7, 127.2, 126.6, 124.8, 121.5, 118.3, 118.0.

5.4.2. 2-(3-Fluorophenyl)-1H-anthra[1,2-d]imidazole-6,11-dione **20**

From 3-fluoro-benzaldehyde (136 mg, 1.1 mmol), **20** was obtained as a yellow solid (177 mg, 0.52 mmol, 52% yield, mp 250–255 °C).

IR (KBr) 3414, 1670, 1647, 1587, 1577, 1529, 1485, 1458, 1328, 1294, 1274, 1188, 713 cm^{-1} ^1H NMR (400 MHz, DMSO-d_6) δ 11.38–11.29 (m, 1H), 8.38–8.33 (m, 1H), 8.32–8.28 (m, 1H), 8.26 (d, *J* = 8.42 Hz, 1H), 8.14 (d, *J* = 8.37 Hz, 1H), 7.96–7.89 (m, 2H), 7.86–7.79 (m, 2H), 7.57 (dd, *J* = 13.61, 7.92 Hz, 1H), 7.31–7.27 (m, 1H). ^{13}C NMR (75 MHz, DMSO-d_6) δ 183.5, 182.8, 164.5, 156.8, 134.9, 134.8, 133.4, 131.7, 131.6, 131.5, 131.4, 131.3, 128.7, 127.2, 126.7, 124.7, 121.5, 118.3, 115.3.

5.4.3. 2-(4-Fluorophenyl)-1H-anthra[1,2-d]imidazole-6,11-dione **21**

From 4-fluoro-benzaldehyde (136 mg, 1.1 mmol), **21** was obtained as a yellow solid (226 mg, 0.66 mmol, 66% yield, mp 280–283 °C).

IR (KBr) 3429, 1670, 1589, 1489, 1330, 1301, 1290, 717 cm^{-1} ^1H NMR (400 MHz, DMSO-d_6) δ 11.38–11.24 (m, 1H), 8.39–8.33 (m, 1H), 8.32–8.28 (m, 1H), 8.26 (d, *J* = 8.36 Hz, 1H), 8.22–8.16 (m, 2H), 8.13 (d, *J* = 8.43 Hz, 1H), 7.86–7.80 (m, 2H), 7.32–7.28 (m, 2H). ^{13}C NMR (75 MHz, DMSO-d_6) δ 183.0, 182.2, 156.6, 164.5, 134.9, 134.8, 134.3, 134.2, 132.9, 130.6, 130.5, 127.9, 126.6, 126.3, 126.1, 125.4, 120.9, 115.8, 115.5.

5.4.4. 2-o-Tolyl-1H-anthra[1,2-d]imidazole-6,11-dione **22**

From 2-methyl-benzaldehyde (132 mg, 1.1 mmol), **22** was obtained as a yellow solid (271 mg, 0.80 mmol, 80% yield, mp 235–239 °C).

IR (KBr) 3346, 1666, 1649, 1575, 1519, 1483, 1438, 1323, 1296, 1008, 840, 773, 727, 713, 648 cm^{-1} ^1H NMR (300 MHz, DMSO-d_6) δ 8.27–8.19 (m, 1H), 8.17–8.10 (m, 2H), 8.04 (d, *J* = 8.38 Hz, 1H), 7.77 (d, *J* = 7.42 Hz, 1H), 7.72–7.66 (m, 2H), 7.38–7.23 (m, 3H), 2.63 (s, 3H). ^{13}C NMR (75 MHz, DMSO-d_6) δ 183.5, 183.0, 159.0, 137.9, 134.9, 134.7, 133.6, 131.3, 131.1, 130.6, 129.9, 128.4, 127.2, 126.7, 126.1, 125.5, 121.1, 21.1.

5.4.5. 2-m-Tolyl-1H-anthra[1,2-d]imidazole-6,11-dione **23**

From 3-methyl-benzaldehyde (132 mg, 1.1 mmol), **23** was obtained as a yellow solid (251 mg, 0.74 mmol, 74% yield, mp 229–231 °C).

IR (KBr) 3444, 1670, 1581, 1525, 1489, 1330, 1290, 713, 684, 354 cm^{-1} ^1H NMR (400 MHz, DMSO-d_6) δ 8.34–8.29 (m, 1H), 8.28–8.23 (m, 1H), 8.21 (d, *J* = 8.37 Hz, 1H), 8.09 (d, *J* = 8.39 Hz, 1H), 7.98 (s, 1H), 7.92 (d, *J* = 7.65 Hz, 1H), 7.82–7.76 (m, 2H), 7.45 (t, *J* = 7.62 Hz, 1H), 7.37 (d, *J* = 7.60 Hz, 1H), 2.49 (s, 3H). ^{13}C NMR (100 MHz, DMSO-d_6) δ 182.8, 183.5, 158.2, 138.5, 134.8, 134.7, 133.5, 132.1, 129.2, 129.1, 128.4, 127.2, 126.6, 125.7, 121.4, 21.4.

5.4.6. 2-(2-Hydroxyphenyl)-1H-anthra[1,2-d]imidazole-6,11-dione **25**

From 2-hydroxy-benzaldehyde (150 mg, 1.1 mmol), **25** was obtained as a yellow solid (174 mg, 0.51 mmol, 51% yield, mp >300 °C).

IR (KBr) 3352, 1664, 1589, 1521, 1487, 1327, 1290, 752, 713 cm^{-1} ^1H NMR (300 MHz, DMSO-d_6) δ 12.68 (s, 1H), 12.11 (s, 1H), 8.32 (d, *J* = 7.4Hz, 1H), 8.14–8.10 (m, 2H), 7.99 (s, 2H), 7.85–7.82 (m, 2H), 7.43–7.37 (ddd, *J* = 7.4 and 1.7Hz, 1H), 7.07–6.97 (m, 2H). ^{13}C NMR (75 MHz, DMSO-d_6) δ 183.6, 182.3, 157.3, 156.3, 134.6, 134.3, 133.2, 133.1, 132.9, 128.8, 127.9, 126.9, 126.3, 123.8, 121.4, 119.8, 117.2, 113.4.

5.4.7. 2-(3-Hydroxyphenyl)-1H-anthra[1,2-d]imidazole-6,11-dione **26**

From 3-hydroxy-benzaldehyde (150 mg, 1.1 mmol), **26** was obtained as a yellow solid (200 mg, 0.59 mmol, 59% yield, mp >300 °C).

IR (KBr) 3530, 3410, 3020, 1658, 1580, 1535, 1488, 1462, 1440, 1325, 1290, 1264, 1234, 1153, 890, 784, 714, 680, 595, 568 cm^{-1} ^1H NMR (300 MHz, DMSO-d_6) δ 12.92 (s, 1H), 9.71 (s, 1H), 8.20–8.16 (m, 2H), 8.09–8.02 (m, 2H), 7.91–7.80 (m, 4H), 7.38 (t, *J* = 7.8 Hz, 1H), 6.99 (dd, *J* = 7.96 and 1.92 Hz, 1H). ^{13}C NMR (75 MHz, DMSO-d_6) δ 183.0, 182.3, 157.8, 157.6, 149.2, 134.4, 134.2, 133.0, 132.9, 132.8, 130.1, 129.8, 127.9, 126.7, 126.2, 124.9, 120.9, 119.1, 118.6, 118.2, 114.9.

5.4.8. 2-(4-Hydroxyphenyl)-1H-anthra[1,2-d]imidazole-6,11-dione **27**

From 4-hydroxy-benzaldehyde (150 mg, 1.1 mmol), **27** was obtained as a yellow solid (187 mg, 0.55 mmol, 55% yield, mp >300 °C).

IR (KBr) 3431, 3134, 1668, 1608, 1585, 1490, 1475, 1458, 1440, 1328, 1295, 1246, 1174, 715 cm^{-1} ^1H NMR (300 MHz, DMSO-d_6) δ 12.78 (s, 1H), 10.06 (s, 1H), 8.27 (d, J = 8.37 Hz, 1H), 8.22–8.17 (m, 3H), 8.06–7.98 (m, 2H), 7.91–7.88 (m, 2H), 6.93 (d, J = 8.78, 2H). ^{13}C NMR (75 MHz, DMSO-d_6) δ 183.2, 182.3, 160.3, 158.2, 149.7, 134.4, 134.2, 133.2, 133.0, 103.1, 127.4, 126.8, 126.2, 124.2, 121.0, 119.8, 118.2, 115.6.

5.4.9. 2-(4-Hydroxy-3-methoxyphenyl)-1H-anthra[1,2-d]imidazole-6,11-dione **28**

From 4-hydroxy-3-methoxy-benzaldehyde (167 mg, 1.1 mmol), **28** was obtained as a yellow solid (258 mg, 0.77 mmol, 77% yield, mp >300 °C).

IR (KBr) 3431, 3331, 1662, 1589, 1490, 1438, 1327, 1290, 1270, 1188, 1165, 1026, 721 cm^{-1} ^1H NMR (400 MHz, DMSO-d_6) δ 11.25–11.25 (s, 1H), 8.37 (dd, J = 6.94, 2.11 Hz, 1H), 8.31 (dd, J = 6.88, 2.14 Hz, 1H), 8.25 (d, J = 8.38 Hz, 1H), 8.11 (d, J = 8.39 Hz, 1H), 7.85–7.80 (m, 3H), 7.62 (dd, J = 8.27, 1.98 Hz, 1H), 7.11 (d, J = 8.24 Hz, 1H), 6.04–6.03 (m, 1H), 4.09–4.07 (s, 3H). ^{13}C NMR (100 MHz, DMSO-d_6) δ 183.6, 182.6, 158.6, 150.1, 148.1, 134.8, 134.6, 133.5, 133.4, 127.8, 127.1, 126.5, 122.4, 121.4, 120.4, 116.0, 112.1, 56.3.

5.5. X-ray analysis

A yellow crystal (0.242 × 0.225 × 0.132 mm^3) of compound **17** was selected for X-ray diffraction. Intensity data were collected at room temperature (T = 298K) using a diffractometer Kappa CCD of Enraf Nonius with MoKα monochromatic radiation (λ = 0.71073 Å) and using the Collect [43] software, as well as Scalepack [44] for cell refinement. For compound **17** a total of 15300 reflections to a maximum 2θ of 25.76° were measured. The crystal structure for compound **17** was solved by direct methods and refined anisotropically with full matrix least square on F^2 using SHELXL-97 program [45]. H atoms attached to C atoms were located on stereochemical grounds placed (C–H = 0.93–0.98 Å) and refined as riding with $U_{iso}(H)$ = 1.5 U_{eq}(C-methyl) or 1.2 U_{eq}(other) times the value of the equivalent isotropic displacement parameter of atoms to which they are bonded. Compound **17** crystallized with two water molecules. The software used were: data collection: COLLECT [43]; cell refinement: HKL SCALEPACK [44]; data reduction: HKL DENZO and SCALEPACK [44]. The program(s) used to solve structure: SHELXS-97 [46]. The program(s) used to refine structure: SHELXL-97 [46] molecular graphics: ORTEP-3 [47], software used to prepare material for publication: WinGX [47]. The main crystallographic parameters were inserted in the supporting information.

Crystallographic data for compound **17** have been deposited with the Cambridge Crystallographic Data Center as Supplementary Publication No. CCDC 742743. Copies of the data can be obtained, free of charge, on application to CCDC, 12 Union Road, Cambridge CH21EZ, UK (fax: +44 1223 336 033 or e-mail: deposit@ccdc.cam.ac.uk).

6. Anticancer assay

6.1. Chemicals

Fetal bovine serum and phytohaemagglutinin were purchased from Cutilab (Campinas, SP, Brazil), and RPMI 1640 medium, trypsin–EDTA, penicillin and streptomycin were purchased from GIBCO® (Invitrogen, Carlsbad, CA, USA). 5-bromo-2′-deoxyuridine, thiobarbituric acid, hydrolyzed 1,1,3,3-tetramethoxypropan, 1-bromoheptane, N-acetylcysteine and colchicine were obtained from Sigma Chemical Co. (St, Louis, MO). Hydrogen peroxide was from Vetec (Brazil). Doxorubicin (Doxolem®) was from Zodiac Produtos Farmacêuticos S/A, Brazil. Low melting point agarose and agarose were obtained from Invitrogen (Carlsbad, CA, USA). All other chemicals and reagents used were of analytical grade.

6.2. Cytotoxicity against cancer cell lines

Compounds (0.01–5 μg/mL) were tested for cytotoxic activity against four cancer cell lines: SF295 (central nervous system), HCT-8 (colon), MDA-MB435 (breast), HL-60 (leukemia) from National Cancer Institute (Bethesda, MD). All cell lines were maintained in RPMI 1640 medium supplemented with 10% fetal bovine serum, 2 mM glutamine, 100 U/mL penicillin, 100 μg/mL streptomycin at 37 °C with 5% CO_2. Each compound was dissolved with DMSO to obtain a concentration of 1 mg/mL. They were incubated with the cells for 72 h. The negative control received the same amount of DMSO (0.1% in the highest concentration). Doxorubicin (0.1–0.58 μg/mL) was used as a positive control. The cell viability was determined by reduction of the yellow dye 3-(4,5-dimethyl-2-thiazol)-2,5-diphenyl-2*H*-tetrazolium bromide (MTT) to a blue formazan product as described by Mosmann [27].

6.3. Inhibition of PBMC proliferation – Alamar Blue assay

To investigate the selectivity of compounds toward a normal proliferating cell, the Alamar Blue assay was performed with peripheral blood mononuclear cells (PBMC) after 72 h of drug exposure. After 24 h, compounds (0.048–25 μg/mL) dissolved in DMSO (0.1%) were added to each well and incubated for 72 h. Doxorubicin (0.01–1.06 μM) was used as positive control. Twenty-four h before the end of the incubation, 10 μL of stock solution (0.312 mg/mL) of the Alamar Blue (Resazurin, Sigma–Aldrich Co) was added to each well. The absorbance was measured using a multiplate reader (DTX 880 Multimode Detector, Beckman Coulter®) and the drug effect was quantified as the percentage of control absorbance at 570 nm and 595 nm. The absorbance of Alamar Blue in culture medium is measured at a higher wavelength and a lower wavelength. The absorbance of the medium is also measured at the higher and lower wavelengths. The absorbance of the medium alone is subtracted from the absorbance of medium plus Alamar Blue at the higher wavelength. This value is called AOHW. The absorbance of the medium alone is subtracted from the absorbance of medium plus Alamar Blue at the lower wavelength. This value is called AOLW. A correction factor, R0, can be calculated from AOHW and AOLW, where R0 = AOLW/AOHW. The percent Alamar Blue reduced is then expressed as follows: % reduced = ALW − (AHW × R0) × 100.

6.4. Cells treatments

Cancer cell lines were treated with compounds (5 μM) during 24 h. Moreover, in order to evaluate the contribution of ROS on the cytotoxicity and genotoxicity of tested compounds, cells were pre-treated for 24 h with 5 mM N-acetylcysteine (NAC) or 50 μM 1-bromoheptane (BH), and after they were exposed to tested compounds (5 μM) during 24 h.

6.5. Cell viability

Cell viability was determined by the trypan blue dye exclusion test in human cancer cell lines. After treatment trypan blue-

excluding cells were counted in a Neubauer chamber, in cell aliquots removed from cultures after 24 h [48].

6.6. Morphological characterization of apoptotic cancer cells

Apoptotic cells were determined at the end of each treatment by use of the acridine-orange (AO)/ethidium-bromide (EB) assay: 25 μL of the cell suspension were mixed with 1 μL of the staining solution (AO 100 μg/mL + EB 100 μg/mL in PBS) and spread on a slide, and 300 cells were counted per data point [49]. The percentage of apoptotic cells was then calculated.

6.7. Alkaline comet assay (single cell gel electrophoresis)

The alkaline comet assay was performed as described by Singh et al. (1988) [50] with minor modifications [51], and following the recommendations of the International Workshop on Genotoxicity Test Procedures [52]. At the end of the treatment, cells were washed with ice-cold PBS, detached with 100 μL trypsin (0.15%) and resuspended in complete RPMI medium. Next, 20 μL of cell suspension ($\sim 10^6$ cells/mL) were mixed with 0.75% low melting point agarose and immediately spread onto a glass microscope slide precoated with a layer of 1% normal melting point agarose. The agarose was allowed to set at 4 °C for 5 min. The slides were incubated in ice-cold lysis solution (2.5 M NaCl, 10 mM Tris, 100 mM EDTA, 1% Triton X-100 and 10% DMSO, pH 10.0) at 4 °C for a minimum of 1 h to remove cellular proteins, leaving the DNA as "nucleoids." After the lysis procedure, the slides were placed on a horizontal electrophoresis unit. The unit was filled with fresh buffer (300 mM NaOH and 1 mM EDTA, pH > 13.0) to cover the slides for 20 min at 4 °C to allow DNA unwinding and expression of alkali-labile sites. Electrophoresis was conducted for 20 min at 25 V and 300 mA (0.86 V/cm). After electrophoresis, the slides were neutralized (0.4 M Tris, pH 7.5), stained with ethidium-bromide (20 μg/mL) and analyzed using a fluorescence microscope. All the above steps were conducted under yellow light or in the dark to prevent additional DNA damage. Images of 100 randomly selected cells (50 cells from each of two replicate slides) were analyzed for each concentration of test substance. Cells were scored visually and assigned to one of five classes, according to tail size (from undamaged-0, to maximally damaged-4), and a damage index value was calculated for each sample of cells. Damage index thus ranged from 0 (completely undamaged: 100 cells × 0) to 400 (with maximum damage: 100 cells × 4) [53].

6.8. Measurement of oxidized purines and pyrimidines

Alkaline comet assay was performed as described above. At the end of the treatment (5 μM during 12 h), slides were removed from the lysing solution, and washed three times in enzyme buffer (40 mM HEPES, 100 mM KCl, 0.5 mM Na_2EDTA, 0.2 mg/mL BSA, pH 8.0), drained, and incubated with 70 μL FPG (30 min 37 °C) or ENDOIII (45 min 37 °C) from New England BioLabs (USA). Images of 100 randomly selected cells (50 cells from each of two replicate slides) were visually analyzed per group. The amount of oxidized purines (FPG-sensitive sites) and pyrimidines (ENDOIII-sensitive sites) was then determined by subtracting the amount of strand breaks (samples incubated with buffer alone) to the total amount of breaks obtained after incubation with FPG and ENDOIII.

6.9. Measurement of lipid peroxidation

The extent of compounds-induced lipid peroxidation was determined by the reaction of thiobarbituric acid (TBA) with malondialdehyde (MDA), a product formed by lipid peroxidation. The assays were performed by according to Salgo and Pryor (1996) [54], with minor modifications. Cancer cells were incubated with compounds (5 μM) for 24 h, and after lysis with Tris–HCl (15 mM for 1 h). Two milliliters 0.4 mg/mL TCA, 0.25 M HCl were added to the lysate, which was then incubated with 6.7 mg/mL thrichloroacetic acid for 15 min at 100 °C. The mixture was centrifuged at 750×*g* for 10 min. As TBA reacts with other products of lipid peroxidation in addition to MDA, results are expressed in terms of thiobarbituric reactive species (TBARS), which are determined by absorbance at 532 nm. Hydrolyzed 1,1,3,3-tetramethoxypropan was used as the standard. The results were normalized by protein content [55].

Conflict of interest

Authors declare no conflict of interest.

Acknowledgments

This research was supported by grants from the Conselho Nacional de Desenvolvimento Científico e Tecnológico (CNPq), Fundação Carlos Chagas Filho de Amparo à Pesquisa do Rio de Janeiro (FAPERJ), CAPES, UnB, UFAL, UFRJ and National Cancer Institute. The authors are also indebted to the PRONEX-FAPERJ (E-26/110.574/2010) and to PRONEX-CNPq-FAPEAL. Dr. Eufrânio N. da Silva Júnior thanks the CNPq for post doctoral financial support (project no. 151558/2009-4).

References

[1] E.A. Hillard, F.C. de Abreu, D.C.M. Ferreira, G. Jaouen, M.O.F. Goulart, C. Amatore, Chem. Commun. (2008) 2612.
[2] (a) E.L. Bonifazi, C. Ríos-Luci, L.G. León, G. Burton, J.M. Padrón, R.I. Misico, Bioorg. Med. Chem. 18 (2010) 2621;
(b) S.B. Ferreira, F.C. da Silva, F.A.F.M. Bezerra, M.C.S. Lourenço, C.R. Kaiser, A.C. Pinto, V.F. Ferreira, Arch. Pharm. 343 (2010) 81.
[3] (a) E.N. da Silva Júnior, R.F.S. Menna-Barreto, M.C.F.R. Pinto, R.S.F. Silva, D.V. Teixeira, M.C.B.V. de Souza, C.A. de Simone, S.L. de Castro, V.F. Ferreira, A.V. Pinto, Eur. J. Med. Chem. 43 (2008) 1774;
(b) N. Kongkathip, B. Kongkathip, P. Siripong, C. Sangma, S. Luangkamin, M. Niyomdecha, S. Pattanapa, S. Piyaviriyagul, P. Kongsaeree, Bioorg. Med. Chem. 11 (2003) 3179.
[4] Y. Su, J. Xie, Y. Wang, X. Hub, X. Lin, Eur. J. Med. Chem. 45 (2010) 2713.
[5] N. Kongkathip, N. Pradidphol, K. Hasitapan, R. Grigg, W.C. Kao, C. Hunte, N. Fisher, A.J. Warman, G.A. Biagini, P. Kongsaeree, P. Chuawong, B. Kongkathip, J. Med. Chem. 53 (2010) 1211.
[6] R.C. Montenegro, A.J. Araújo, M.T. Molina, J.D.B.M. Filho, D.D. Rocha, E. Lopéz-Montero, M.O.F. Goulart, E.S. Bento, A.P.N.N. Alves, C. Pessoa, M.O. de Moraes, L.V. Costa-Lotufo, Chem. Biol. Interact. 184 (2010) 439.
[7] E. Pérez-Sacau, R.G. Díaz-Peñate, A. Estévez-Braun, A.G. Ravelo, J.M. García-Castellano, L. Pardo, M. Campillo, J. Med. Chem. 50 (2007) 696.
[8] A.I. Francisco, A. Casellato, A.P. Neves, J.W.M. Carneiro, M.D. Vargas, L.C. Visentin, A. Magalhães, C.A. Câmara, C. Pessoa, L.V. Costa-Lotufo, J.D.B.M. Filho, M.O. de Moraes, J. Braz. Chem. Soc. 21 (2010) 169.
[9] A.I. Francisco, M.D. Vargas, T.P. Fragoso, J.W.M. Carneiro, A. Casellato, F.C. da Silva, V.F. Ferreira, J.P. Barbosa, C. Pessoa, L.V. Costa-Lotufo, J.D.B.M. Filho, M.O. de Moraes, A.S. Mangrich, J. Braz. Chem. Soc. 21 (2010) 1293.
[10] L.M. Lima, E.J. Barreiro, Curr. Med. Chem. 12 (2005) 23.
[11] C. Viegas Jr., A.C. Danuello, V.S. Bolzani, E.J. Barreiro, C.A.M. Fraga, Curr. Med. Chem. 14 (2007) 1829.
[12] (a) M.V. Gil, M.J. Arevalo, O. Lopez, Synthesis 11 (2007) 1589;
(b) H.C. Kolb, M.G. Finn, K.B. Sharpless, Angew. Chem. Int. Ed. 40 (2001) 2004.
[13] Y.A. Al-Soud, N.A. Al-Masoudi, A. El-Rahman, S. Ferwanah, Bioorg. Med. Chem. 11 (2003) 1701.
[14] E.N. da Silva Júnior, M.A.B.F. de Moura, A.V. Pinto, M.C.F.R. Pinto, M.C.B.V. de Souza, A.J. Araújo, C. Pessoa, L.V. Costa-Lotufo, R.C. Montenegro, M.O. de Moraes, V.F. Ferreira, M.O.F. Goulart, J. Braz. Chem. Soc. 20 (2009) 635.
[15] E.N. da Silva Júnior, M.C.B.V. de Souza, A.V. Pinto, M.C.F.R. Pinto, M.O.F. Goulart, F.W.A. Barros, C. Pessoa, L.V. Costa-Lotufo, R.C. Montenegro, M.O. de Moraes, V.F. Ferreira, Bioorg. Med. Chem. 15 (2007) 7035.
[16] E.N. da Silva Júnior, C.F. de Deus, B.C. Cavalcanti, C. Pessoa, L.V. Costa-Lotufo, R.C. Montenegro, M.O. de Moraes, M.C.F.R. Pinto, C.A. de Simone, V.F. Ferreira, M.O.F. Goulart, C.K.Z. Andrade, A.V. Pinto, J. Med. Chem. 53 (2010) 504.
[17] M.G. Ettlinger, J. Am. Chem. Soc. 72 (1950) 3472.
[18] A.Y. Yakubovskaya, T.Y. Kochergina, V.A. Denisenko, D.V. Berdyshev, V.P. Glazunov, V.P. Anufriev, Russ. Chem. Bull. Int. Ed. 55 (2006) 301.
[19] E.N. da Silva Júnior, M.C.F.R. Pinto, K.C.G. de Moura, C.A. de Simone, C.J. Nascimento, C.K.Z. Andrade, A.V. Pinto, Tetrahedron Lett. 50 (2009) 1575.

[20] E.N. da Silva Júnior, T.T. Guimarães, R.F.S. Menna-Barreto, M.C.F.R. Pinto, C.A. de Simone, C. Pessoa, B.C. Cavalcanti, J.R. Sabino, C.K.Z. Andrade, M.O.F. Goulart, S.L. de Castro, A.V. Pinto, Bioorg. Med. Chem. 18 (2010) 3224.
[21] M.C.F.R. Pinto, A.V. Pinto, C.G.T. Oliveira, An. Acad. Brasil. Ciências 52 (1980) 481.
[22] L.F. Fieser, M. Fieser, J. Am. Chem. Soc. 70 (1948) 3215.
[23] X. Peng, Y. Wu, J. Fan, M. Tian, K. Han, J. Org. Chem. 25 (2005) 10524.
[24] F.S. Cruz, B. Gilbert, J.N. Lopes, R. Pinchin, A.V. Pinto, Rev. Latinoamer. Quim 8 (1977) 140.
[25] (a) C.W. Tornøe, C. Christiensen, M. Meldal, J. Org. Chem. 67 (2002) 3057;
(b) V.V. Rostovtsev, G.L. Green, V.V. Fokin, K.B. Sharpless, Angew. Chem. Int. Ed. 41 (2002) 2596.
[26] T.T. Guimarães, E.N. da Silva Júnior, C.E.M. Carvalho, C.A. de Simone, A.V. Pinto, Acta Crystallogr. E65 (2009) o1063.
[27] T. Mosmann, J. Immunol. Methods 65 (1983) 55.
[28] (a) H. Louise, W. Jordana, G. Renate, A.R. John, Drug Metab. Lett. 1 (2007) 245;
(b) S. Subramanian, M.M.C. Ferreira, M. Trsic, Struct. Chem. 9 (1998) 47.
[29] A. Koceva-Chyla, B. Wieclawska, Z. Józwiak, M. Bryszewska, Cell Biol. Int. 30 (2006) 645.
[30] E.K. Choi, K. Terai, I.M. Ji, Y.H. Kook, K.H. Park, E.T. Oh, R.J. Griffin, B.U. Lim, J.S. Kim, D.S. Lee, D.A. Boothman, M. Loren, C.W. Song, H.J. Park, Neoplasia 9 (2007) 634.
[31] H.E. Poulsen, Exp. Toxicol. Pathol. 57 (2005) 161.
[32] (a) D.W. Nicholson, Nature 407 (2000) 810;
(b) M. Bamford, G. Walkinshaw, R. Brown, Exp. Cell Res. 256 (2000) 1;
(c) J.L. Fernandez-Luna, Clin. Transl. Oncol. 9 (2007) 555.
[33] S. Khan, P.J. O'Brien, Biochem. Biophys. Res. Commun. 179 (1991) 436.
[34] (a) A.S. Park, K.S. Choi, J.H. Bang, K. Huh, S.U. Kim, J. Neurochem. 75 (2000) 946;
(b) N. van Zandwij, Chest 107 (1995) 1437.
[35] (a) K. Ollinger, A. Brunmark, J. Biol. Chem. 266 (1991) 21496–21503;
(b) R. Zangh, O. Hirsch, M. Mohsen, A. Samuni, Arch. Biochem. Biophys. 312 (1994) 385–391;
(c) P.H. Lin, W.C. Pan, Y.W. Kang, Y.L. Chen, C.H. Lin, M.C. Lee, Y.H. Chou, J. Nakamura, Chem. Res. Toxicol. 18 (2005) 1262–1270.
[36] S. Bjelland, E. Seeberg, Mutat. Res. 531 (2003) 37–80.
[37] (a) G. Speit, P. Schutz, I. Bonzheim, K. Trenz, H. Hoffmann, Toxicol. Lett. 146 (2004) 151–158;
(b) A.R. Collins, S.J. Duthie, V.L. Dobson, Carcinogenesis 14 (1993) 1733–1735.
[38] M. Valko, D. Leibfritz, J. Moncol, M.T. Cronin, M. Mazur, J. Telser, Int. J. Biochem. Cell Biol. 39 (2007) 44–84.
[39] C.C. Smith, M.R. O'Donovan, E.A. Martin, Mutagenesis 21 (2006) 185–190.
[40] H. Ide, Prog. Nucleic Acid Res. Mol. Biol. 68 (2001) 207–221.
[41] G.D. Buffiton, K. Ollinger, A. Brunmark, E. Cadenas, Biochem. J. 257 (1989) 561–571.
[42] (a) A.B. Pardee, Y.Z. Li, C.J. Li, Curr. Cancer Drug Targets 2 (2002) 227–242;
(b) A. Esteves-Souza, K.A. Lucio, A.S. da Cunha, A.C. Pinto, E.L.S. Lima, C.A. Camara, M.D. Vargas, C.R. Gattass, Oncol. Rep. 20 (2008) 225–231;
(c) D.C.M. Ferreira, M.O.F. Goulart, M.S.A. Moreira, A.V. Pinto, I. Tapsoba, S. Arbault, C. Amatore, ChemBioChem. 10 (2009) 528–538;
(d) B.K. Aithal, M.R. Kumar, B.N. Rao, N. Udupa, B.S. Rao, Cell Biol. Int. 33 (2009) 1039–1049;
(e) R.J. McKallip, C. Lombard, J. Sun, Toxicol. Appl. Pharmacol. 247 (2010) 41–52;
(f) V. Klaus, T. Hartmann, J. Gambini, P. Graf, W. Stahl, A. Hartwig, L.O. Klotz, Arch. Biochem. Biophys. 496 (2010) 93–100.
[43] Enraf-Nonius, COLLECT. Nonius BV, Delft, The Netherlands, 1997–2000.
[44] Z. Otwinowski, W. Minor, H.K.L. Denzo and Scalepack. in: C.W. Carter Jr., R.M. Sweet (Eds.), Methods in Enzymology, vol. 276. Academic Press, New York, 1997, pp. 307–326.
[45] G.M. Sheldrick, SHELXL-97. Program for Crystal Structures Analysis. Univ. of Göttingen, Göttingen, Germany, 1997.
[46] G.M. Sheldrick, SHELXS-97. Program for Crystal Structure Resolution. Univ. of Göttingen, Göttingen, Germany, 1997.
[47] L.J. Farrugia, J. Appl. Crystallogr. 30 (1997) 565 ORTEP3 for Windows.
[48] B.C. Cavalcanti, H.V.N. Júnior, M.H.R. Seleghim, R.G.S. Berlinck, G.M.A. Cunha, M.O. Moraes, C. Pessoa, Chem. Biol. Interact. 174 (2008) 155.
[49] B.C. Cavalcanti, D.P. Bezerra, H.I.F. Magalhães, M.O. Moraes, A.S. Lima, E.R. Silveira, C.A.G. Câmara, V.S. Rao, C. Pessoa, L.V. Costa-Lotufo, J. Appl. Toxicol. 29 (2009) 560.
[50] N.P. Singh, M.T. McCoy, R.R. Tice, E.L. Scheider, Exp. Cell Res. 175 (1988) 184.
[51] A. Hartmann, G. Speit, Toxicol. Lett. 90 (1997) 183.
[52] R.R. Tice, E. Agurell, D. Anderson, B. Burlinson, A. Hartmann, H. Kobayashi, Y. Miyamae, E. Rojas, J.C. Ryu, Y.F. Sasaki, Environ. Mol. Mutagen. 35 (2000) 206.
[53] B.C. Cavalcanti, J.R.O. Ferreira, D.J. Moura, R.M. Rosa, G.V. Furtado, R.R. Burbano, E.R. Silveira, M.A.S. Lima, C.A.G. Camara, J. Saffi, J.A.P. Henriques, V.S.N. Rao, L.V. Costa-Lotufo, M.O. Moraes, C. Pessoa, Mutat. Res. 701 (2010) 153.
[54] M.G. Salgo, W.A. Pryor, Arch. Biochem. Biophys. 333 (1996) 482–488.
[55] O.H. Lowry, N.J. Rosebrough, A.L. Farr, R.J. Randall, J. Biol. Chem. 193 (1951) 265–275.